## Random matrix model for quantum dots with interactions and the conductance peak spacing distribution

Y. Alhassid, Ph. Jacquod and A. Wobst Center for Theoretical Physics, Sloane Physics Laboratory, Yale University, New Haven, Connecticut 06520, USA (September 19, 2018)

We introduce a random interaction matrix model (RIMM) for finite-size strongly interacting fermionic systems whose single-particle dynamics is chaotic. The model is applied to Coulomb blockade quantum dots with irregular shape to describe the crossover of the peak spacing distribution from a Wigner-Dyson to a Gaussian-like distribution. The crossover is universal within the random matrix model and is shown to depend on a single parameter: a scaled fluctuation width of the interaction matrix elements. The crossover observed in the RIMM is compared with the results of an Anderson model with Coulomb interactions.

PACS numbers: 73.23.Hk, 05.45+b, 73.20.Dx, 73.23.-b

The transport properties of semiconductor quantum dots can be measured by connecting the dots to leads via point contacts [1]. When these point contacts are pinched off, effective barriers are formed between the dot and the leads, and the charge on the dot is quantized. Adding an electron to the dot requires a charging energy  $E_C$  to overcome the Coulomb repulsion with electrons already in the dot. This repulsion can be compensated by modifying the gate voltage  $V_g$  on the dot. For temperatures below  $E_C$ , a series of Coulomb blockade oscillations is observed in the linear conductance as a function of  $V_g$ . For temperatures much smaller than the mean level spacing  $\Delta$ , the conductance is dominated by resonant tunneling and the Coulomb blockade oscillations become a series of sharp peaks.

In dots with irregular shapes, the classical single-electron dynamics is mostly chaotic. Quantum mechanically, chaotic systems are expected to exhibit universal fluctuations that are described by random matrix theory (RMT). The distributions [2] and parametric correlations [3] of the Coulomb blockade peak heights in quantum dots have been derived using RMT, and these predictions have been confirmed experimentally [4,5].

Another quantity of recent experimental and theoretical interest is the peak spacing statistics. The peak spacing  $\Delta_2$  can be expressed as a second order difference of the ground state energy  $\mathcal{E}_{g,s}^{(n)}$  of the *n*-electron dot as a function of the number of electrons:

$$\Delta_2 = \mathcal{E}_{g.s.}^{(n+1)} + \mathcal{E}_{g.s.}^{(n-1)} - 2\mathcal{E}_{g.s.}^{(n)}.$$
(1)

Using the constant interaction model (which ignores interactions except for a classical Coulomb energy of  $n^2E_C/2$ ), and assuming a single-particle spectrum that

is independent of n,  $\Delta_2 = E_{n+1} - E_n + E_C$ , where  $E_n$ is the *n*-th single-particle energy. Within this model, RMT suggests a Wigner-Dyson distribution of the peak spacings with a width of  $\sim \Delta/2$ . However recent experiments find a distribution that is Gaussian-like and has a larger width [6–9]. This observation underlines the limitations of the constant interaction model and the importance of electron-electron interactions beyond an average Coulomb energy. Some observed features of the peak spacing distribution have been reproduced using exact numerical diagonalization of small disordered dots  $(n \lesssim 10)$  with Coulomb interactions [6,10]. The width of the distribution is found to increase monotonically with the gas parameter  $r_s$ . Analytic RPA estimates in a disordered dot for small values of  $r_s$  give peak spacing fluctuations that are larger than those of RMT but still of the order of  $\Delta$  [11]. Recent Hartree-Fock calculations [12,13] of larger disordered and chaotic dots with interactions (up to  $n \sim 50$  electrons) also reproduce Gaussian-like peak spacing distributions.

The above studies were carried out for particular models of quantum dots using Coulomb as well as nearestneighbor interactions, and it is not clear how generic the conclusions are. It is also not obvious which bare electron-electron interaction should be taken to represent the experiments because of screening generated by external charges. It is therefore important to find out whether the observed statistics of the peak spacings is generic, and in particular whether it can be reproduced by a modified random matrix model. Standard RMT does not make explicit reference to interactions or to number of particles. To study generic interaction effects on the statistics, we need a random matrix model in which the two-body interactions are distinguished from the one-body part of the Hamiltonian. Recently a two-body random interaction model (TBRIM) introduced in nuclear physics [14] was used together with a diagonal random one-body Hamiltonian to study thermalization in finite-size systems [15] and the crossover from Poisson to Wigner-Dyson statistics in many-body systems [16]. The model explains statistical features observed in atomic [17] and nuclear [18] shell model calculations. However, the Poisson statistics that was used as a non-interacting limit of the model [16,17] is not suitable for the study of dots whose singleelectron dynamics is chaotic.

In this paper we introduce a random interaction matrix model (RIMM) for strongly interacting Fermi sys-

tems whose single-particle dynamics is chaotic. With this model we can study generic and universal effects associated with the interplay of one-body chaos and two-body interactions. In particular, we apply the model to study the peak spacing statistics and find a crossover from a Wigner-Dyson distribution to a Gaussian-like distribution as a function of a parameter that measures the fluctuations of the interaction matrix elements. The crossover depends on both the number of particles and the number of single-particle orbits but becomes universal upon an appropriate scaling of the interaction strength. The crossover is demonstrated in a model of a small disordered dot with Coulomb interactions, and we show that the results can be scaled approximately onto those of the RIMM.

A general Hamiltonian for spinless interacting fermions has the form

$$H = \sum_{ij} h_{ij} a_i^{\dagger} a_j + \frac{1}{4} \sum_{ijkl} \bar{u}_{ijkl} a_i^{\dagger} a_j^{\dagger} a_l a_k , \qquad (2)$$

where  $h_{ij}$  are the matrix elements of the one-body Hamiltonian and  $\bar{u}_{ij;kl} = \langle ij|u|kl\rangle - \langle ij|u|lk\rangle$  are the antisymmetrized matrix elements of the two-body interaction. The states  $|i\rangle = a_i^{\dagger}|0\rangle$  describe a fixed basis of m single-particle states. We define an ensemble of random matrices H of the form (2), where the one-body  $m \times m$  matrix  $h_{ij}$  belongs to the Gaussian ensemble of symmetry class  $\beta$ , and the matrix elements of the two-body interaction are real independent Gaussian variables with zero average and variance  $U^2$  ( $\frac{1}{2}U^2$ ) for the diagonal (off-diagonal) elements

$$P(h) \propto e^{-\frac{\beta}{2a^2} \text{Tr } h^2} \; ; \quad P(\bar{u}) \propto e^{-\text{Tr } \bar{u}^2/2U^2} \; ,$$
 (3)

Eqs. (2) and (3) define the RIMM. The parameter a determines the single-particle level spacing  $\Delta$ . In the non-interacting limit U=0, the random ensemble describes the universal statistical properties of a system whose single-particle dynamics is chaotic. For conserved time-reversal symmetry h is a GOE matrix, while for broken time-reversal symmetry, e.g. in presence of an external magnetic field, h becomes a GUE matrix. The random ensemble for the two-body part of the Hamiltonian (2) is invariant under orthogonal transformations of the single-particle basis. An average interaction that is invariant under such transformations can be included in the model, but it leads to a constant charging energy shift in  $\Delta_2$  and does not affect the peak spacing statistics.

The randomness of the two-body interaction matrix elements is motivated by the strong fluctuations of the Coulomb interaction matrix elements in the basis of eigenstates of the chaotic single-particle Hamiltonian. The RIMM differs from the TBRIM [15,16] in its one-body part, which is less relevant at the high excitation energies considered in the earlier studies but is of crucial importance near the ground state. The TBRIM has a

Poissonian statistics in the non-interacting limit, in contrast to the Wigner-Dyson statistics characterizing the non-interacting limit of (2). Our random interaction matrix model is suitable for describing the generic statistical fluctuations in quantum dots with chaotic single-particle dynamics and in the presence of electron-electron interactions. The model depends on three parameters:  $U/\Delta$ , the number of single-particle orbits m, and the number of particles n.

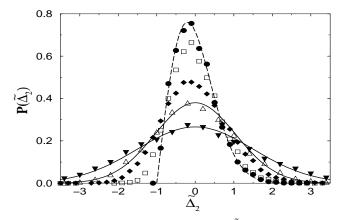


FIG. 1. Peak spacing distributions  $P(\tilde{\Delta}_2)$  for the random matrix model (2) for  $m=12,\ n=4$  and for  $U/\Delta=0$  (solid circles), 0.35 (open squares), 0.7 (solid diamonds), 1.1 (open triangles) and 1.8 (solid triangles). The one-body part h is a GOE. We see a crossover from a Wigner-Dyson distribution for U=0 (dashed line) to Gaussian-like distributions for  $U/\Delta\gtrsim 1$ . The solid lines are Gaussian distributions with the widths of the  $U/\Delta=1.1$  and 1.8 distributions, respectively.

Next we apply the RIMM(2) to study the peak spacing statistics in Coulomb blockade quantum dots. Peak spacings are computed using (1); i.e. the ground-state energy is calculated for three consecutive numbers of particles n-1, n and n+1, and statistics are collected by generating realizations of the ensemble H.

Typical distributions of  $\tilde{\Delta}_2 \equiv (\Delta_2 - \langle \Delta_2 \rangle)/\Delta$  for the case of conserved time-reversal symmetry (h is a GOE matrix) are shown in Fig. 1 for several values of  $U/\Delta$ . For the non-interacting case we obtain the Wigner-Dyson distribution (dashed line), but as  $U/\Delta$  increases a crossover is observed to a Gaussian-like distribution. The distributions for  $U/\Delta = 1.1$  and 1.8 are compared with a Gaussian of the same width (solid lines). The model (2) does not include spin and therefore cannot reproduce the expected bimodal structure of the peak spacing distribution at weak interactions. However, numerical simulations in small disordered dots indicate that this bimodal structure disappears already for weak interactions [10].

The standard deviation of the spacing fluctuations  $\sigma(\tilde{\Delta}_2)$  (in units of  $\Delta$ ) is shown in the top panel of Fig. 2 vs.  $U/\Delta$  for n=4 and several values of m. The statistical errors (due to finite number of samples) are also estimated but are smaller than the size of the symbols.

At zero interaction we are close to the GOE value of  $\approx 0.52$ .  $\sigma(\tilde{\Delta}_2)$  increases slowly and then more rapidly above  $U/\Delta \sim 0.5$ . At strong interactions it is approximately linear in  $U/\Delta$ . The top inset of Fig. 2 shows similar curves of the spacing fluctuations but for constant number of single-particle states m=14 and for several values of n. The standard deviation curve versus  $U/\Delta$  depends on both m and n. However upon the linear scaling  $U_{\rm eff}=f(m,n)U/\Delta$  (f(m,n) is a scaling constant) all curves coalesce to a single universal curve.

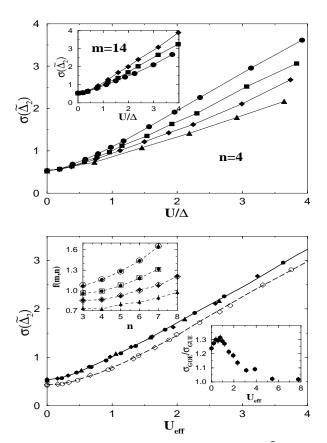


FIG. 2. Top panel: the standard deviation  $\sigma(\tilde{\Delta}_2)$  of the peak spacing fluctuations as a function of  $U/\Delta$  for the random matrix model (2) with a GOE h. Shown are curves for n = 4 and m = 10 (circles), 12 (squares), 14 (diamonds) and 16 (triangles). Top inset: similar curves for m = 14and n=4 (circles), 6 (squares) and 8 (diamonds). Bottom panel: The same curves as in the top panel but as a function of  $U_{\text{eff}} = f(m, n)U/\Delta$ . The curves are shown by their corresponding solid symbols except for the reference curve (m = 12, n = 4) which is shown by a solid line. Similar scaled curves (n = 4 and m = 10, 14) are shown for the GUE case (open symbols) and compared with the GUE reference curve (dashed line). Left inset: the scaling factors f(m,n)as a function of n for the GOE (solid symbols) and the GUE (open symbols) for m = 10, 12, 14 and 16 (from top to bottom). Bottom inset: the ratio  $\sigma_{\text{GOE}}(\hat{\Delta}_2)/\sigma_{\text{GUE}}(\hat{\Delta}_2)$  versus  $U_{\text{eff}}$  calculated using the m=12, n=4 data.

To demonstrate the scaling we first choose a 'reference'

curve, e.g., m=12 and n=4, which we determine accurately using 10,000 realizations at each value of  $U/\Delta$ . For other values of (m,n) we use typically  $\sim 1000-5000$  realizations and find the scaling factors f(m,n) by a least squares fit. The bottom panel of Fig. 2 shows the same curves of the top panel (solid symbols) in comparison with the reference curve (solid line), but as a function of the scaled parameter  $U_{\rm eff}$ . The curves scale almost perfectly within the statistical errors. Also shown are scaled GUE curves (open symbols) for n=4 in comparison with the GUE reference curve (dashed line).

The scaling factor f(m,n) is shown in the left inset of the bottom panel of Fig. 2 as a function of n for different values of m and for both the GOE (solid symbols with error bars) and the GUE (large open symbols) cases. Within the statistical errors f(m,n) is independent of the symmetry class, supporting the universality of our model.

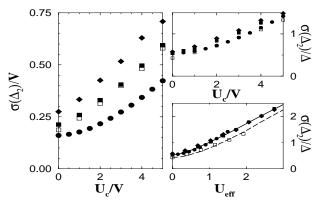


FIG. 3. Left panel:  $\sigma(\Delta_2)$  versus  $U_c/V$  for a  $4\times 5$  cylindrical Anderson lattice with Coulomb interactions. Shown are curves for  $\Phi=0$  and a disorder strength of W=3,5,7 (solid circles, squares and diamonds, respectively), and for  $\Phi=0.15\Phi_0$  and W=5 (open squares). Right top panel:  $\sigma(\Delta_2)/\Delta$  versus  $U_c/V$  for the same cases shown on the left panel. Notice the weak dependence on W. Right bottom panel:  $\sigma(\Delta_2)/\Delta$  for the Coulomb model (symbols) versus the scaled  $U_{\rm eff}=c_0U_c/V$  in comparison with the reference curves of the GOE (solid) and GUE (dashed) random matrix model.

The width of the spacing distribution is larger for the GOE case than for the GUE case at any value of  $U_{\rm eff}$ . The bottom right inset of Fig. 2 is the ratio  $\sigma_{\rm GOE}(\tilde{\Delta}_2)/\sigma_{\rm GUE}(\tilde{\Delta}_2)$  versus  $U_{\rm eff}$ , calculated from the reference curves. The ratio is  $\sim 1.24 \pm 0.02$  for the non-interacting case (in close agreement with the RMT value), and depends only weakly on the interaction in the crossover regime  $U_{\rm eff}\lesssim 1$ . This is consistent with recent measurements [8] which find a ratio of  $\sim 1.2-1.3$  for semiconductor quantum dots with a gas constant of  $r_s \sim 1-2$ . At stronger interactions the ratio decreases. At large values of U, the two-body Hamiltonian dominates and one can ignore the one-body part. Since it is only the latter that distinguishes between the conserved

and broken time-reversal symmetry cases, the ratio of the widths approaches 1 at strong interactions.

Next we compare the crossover observed in the RIMM to the results for a tight-binding Anderson model with cylindrical geometry, hopping parameter V=1, and onsite disorder with a box distribution of width W. Electrons at different sites interact via a Coulomb interaction whose strength is  $U_c = e^2/a$  over one lattice constant a. The standard deviation of the peak spacing  $\sigma(\Delta_2)$  is shown in the left panel of Fig. 3 versus  $U_c/V$  for a  $4\times5$ lattice, n = 4 electrons and several values of W. The values of W are chosen so that the RMT statistics is approximately satisfied in the non-interacting case. In the absence of a magnetic field we choose W = 3, 5, 7. However, in the presence of a magnetic flux, which we apply inside the cylinder and incorporate in the hopping matrix elements in the perpendicular direction ( $\Phi = 0.15\Phi_0$ ), only the W = 5 case satisfies the spectral RMT statistics. We find that  $\sigma_{B=0}(\Delta_2)$  is monotonically increasing with W. After rescaling  $\sigma$  by the mean level spacing  $\Delta$  at the Fermi energy, the residual W-dependence of  $\sigma(\Delta_2)/\Delta$  is rather weak (top right panel of Fig. 3). The standard deviation curves for the Coulomb model can be mapped approximately on the random matrix model curve (bottom right panel of Fig. 3) by defining  $U_{\text{eff}} = c_0 U_c / V$  for some constant  $c_0$  that depends on the disorder strength and lattice size.  $c_0$  depends only weakly on W.

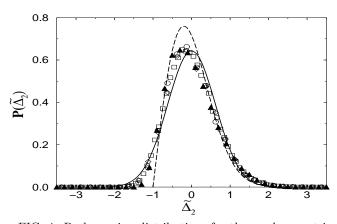


FIG. 4. Peak spacing distributions for the random matrix model (2) (where h is a GOE matrix) for  $m=10,\ n=6,\ U/\Delta=0.24$  (open circles);  $m=12,\ n=4,\ U/\Delta=0.33$  (open squares), and  $m=14,\ n=4,\ U/\Delta=0.42$  (open diamonds). In all three cases  $U_{\rm eff}=0.33$ . The solid triangles show the peak spacing distribution of the Coulomb model for n=4 electrons on a  $4\times 5$  lattice with W=5 and  $U_c/V=0.75$ .

The universal aspects of the crossover can also be investigated by studying the peak spacing distributions themselves. In Fig. 4 we show the peak spacing distributions for three different values of (m,n) but at constant  $U_{\rm eff}=0.33$  (corresponding to three different values of  $U/\Delta$ ). We find that all three distributions coincide, indicating that finite size effects in the random ma-

trix model are negligible. A corresponding distribution for the Coulomb model is also shown for  $U_c/V=0.75$ , W=5 and n=4 and is rather close to the random matrix model distributions. The deviations seen in the Coulomb case may be partly due to finite size effects that are non-universal; even at  $U_c=0$  we observe deviations from the expected Wigner-Dyson distribution.

In conclusion, we showed that a random interaction matrix model that includes a one-body part belonging to one of the standard Gaussian ensembles and a two-body random interaction is suitable for studying generic interaction effects on the statistics of finite Fermi systems whose single-particle dynamics is chaotic. We applied the model to chaotic dots in the Coulomb blockade regime, where it describes a crossover of the peak spacing statistics from a Wigner-Dyson to a Gaussian-like distribution.

This work was supported in part by the U.S. Department of Energy grant No. DE-FG-0291-ER-40608 and the Swiss National Science Foundation. A.W. acknowledges financial support from the Studienstiftung des deutschen Volkes.

- [1] M.A. Kastner, 1992, Rev. Mod. Phys. 64, 849.
- [2] R.A. Jalabert, A.D. Stone, and Y. Alhassid, Phys. Rev. Lett. 68, 3468 (1992).
- [3] Y. Alhassid and H. Attias, Phys. Rev. Lett. 76, 1711 (1996).
- [4] A. M. Chang et. al., Phys. Rev. Lett. 76, 1695 (1996).
- [5] J. A. Folk et. al., Phys. Rev. Lett. 76, 1699 (1996).
- [6] U. Sivan et. al., Phys. Rev. Lett. 77, 1123 (1996).
- [7] F. Simmel, T. Heinzel and D. A. Wharam, Europhys. Lett. 38, 123 (1997).
- [8] S.R. Patel et. al., Phys. Rev. Lett. 80, 4522 (1998).
- [9] F. Simmel et. al., Phys. Rev. B **59**, R 10441 (1999).
- [10] R. Berkovits, Phys. Rev. Lett. 81, 2128 (1998).
- [11] Ya. M. Blanter, A.D. Mirlin, and B.A. Muzykantskii, Phys. Rev. Lett. 78, 2449 (1997).
- 12] S. Levit and D. Orgad, Phys. Rev. B **60**, 5549 (1999).
- [13] P.N. Walker, G. Montambaux and Y. Gefen, Phys. Rev. B 60, 2541 (1999); A. Cohen, K. Richter and R. Berkovits, Phys. Rev. B 60, 2536 (1999).
- [14] J.B. French and S.S.M. Wong, Phys. Lett. B 33, 449 (1970); 35, 5(1971); O. Bohigas and J. Flores, Phys. Lett. B 4, 261 (1971); 35, 383 (1971).
- [15] V.V. Flambaum, G.F. Gribakin and F.M. Izrailev, Phys. Rev. E 53, 5729 (1996).
- [16] Ph. Jacquod, and D.L. Shepelyansky, Phys. Rev. Lett. 79, 1837 (1997); S. Åberg, Phys. Rev. Lett. 64, 3119 (1990).
- [17] V.V. Flambaum et. al., Phys. Rev. A 50, 267 (1994).
- [18] V. Zelevinsky, B.A. Brown, N. Frazier and M. Horoi, Phys. Rep. 276, 85 (1996).